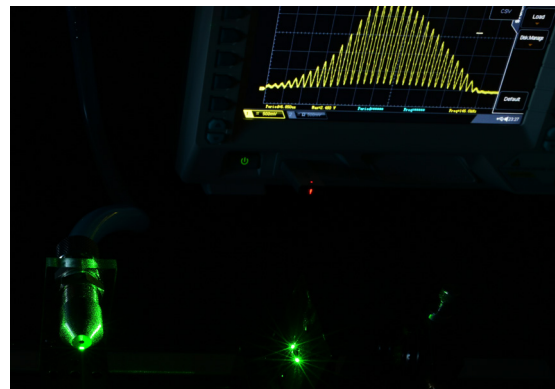
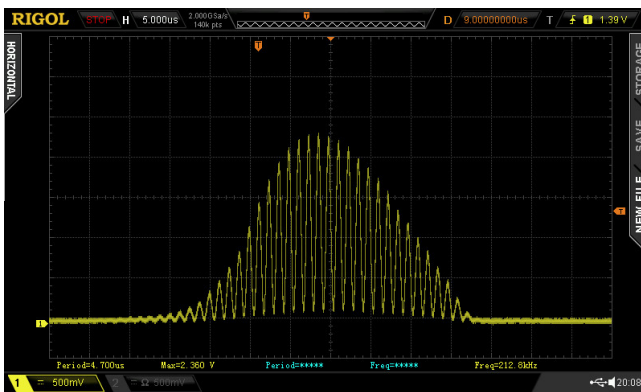
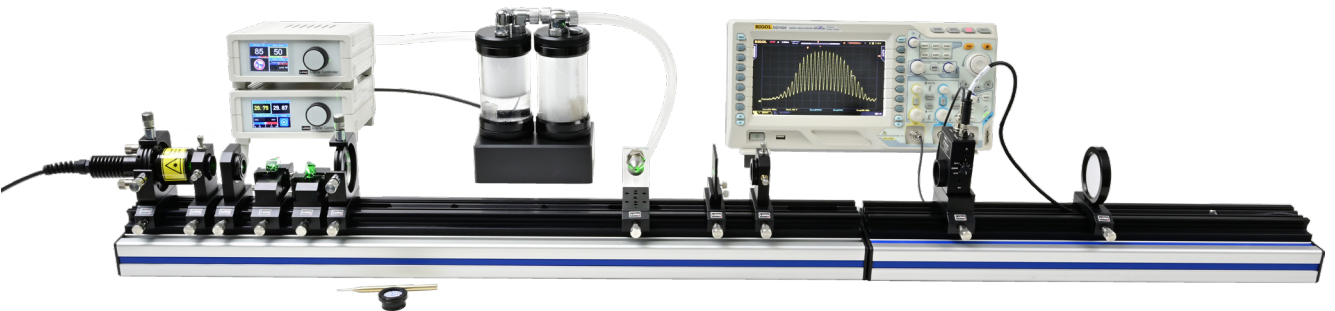


# Manual LM-05 LDA Laser Doppler Anemometer



# Table of Contents

<b>1.0 INTRODUCTION</b>	<b>3</b>
<b>2.0 INTERFERENCE OF TWO GAUSSIAN BEAMS</b>	<b>4</b>
2.1 <i>Gaussian beam properties</i>	4
2.2 <i>Gaussian beam interference</i>	5
2.3 <i>Fringe spacing</i>	6
<b>3.0 DESCRIPTION OF THE COMPONENTS</b>	<b>7</b>
3.1 <i>Optical rail (A,B)</i>	7
3.2 <i>LQ-0040 532 nm stabilized Laser (1)</i>	7
3.3 <i>Beam expander (2,3)</i>	7
3.4 <i>Beam splitter unit (4)</i>	8
3.5 <i>Beam bender unit (5)</i>	8
3.6 <i>Focusing and bending lens (6)</i>	8
3.7 <i>Jet stream module (7)</i>	8
3.8 <i>Beam alignment aid (8)</i>	8
3.9 <i>Imaging lens (9)</i>	9
3.10 <i>Display Screen (12)</i>	9
3.11 <i>Crossed hair target screen (11)</i>	9
3.12 <i>Fast photodetector (10)</i>	9
3.13 <i>LDA Particle Generator (13)</i>	9
3.14 <i>DC-0320 US particle generator</i>	10
3.15 <i>Digital Diode Laser Controller (14)</i>	10
3.15.1 Diode laser controller screens	11
3.15.2 Laser Safety	11
3.15.3 Diode Laser Settings	11
3.15.4 Modulation settings	11
<b>4.0 SET-UP AND ALIGNMENT</b>	<b>13</b>
<b>5.0 MEASUREMENTS</b>	<b>17</b>
5.1 <i>Example of Measurements</i>	17

## 1.0 Introduction

When children play by striking the vertical bars of a picket fence with a stick, they produce a characteristic burst-like noise. The faster they run, the shorter the burst of sound, but the frequency of the strikes increases.

In 1964, Yeh and Cummins utilized a similar principle to invent the Laser Doppler Anemometer (LDA). The word „anemos“ comes from Greek and means “wind.” Therefore, a Laser Doppler Anemometer can be thought of as a “wind meter” that uses laser technology. However, the LDA does not detect pure wind as a clean air stream; it requires particles to be present in the wind. These particles are directed to pass through two intersecting laser beams generated from a single source. Due to the coherence of the laser, a spatial interference pattern resembling zebra stripes emerges in the crossing zone. As particles move through these stripes, they scatter the light in specific directions.

Instead of children playing, this setup employs an ultrasonic particle generator. Through a nozzle, the “dry” water particles are introduced perpendicularly into the interference zone. A photodetector connected to a fast and sensitive amplifier is used to detect the scattered light. A storage oscilloscope is then necessary to display and store the individual bursts for subsequent analysis.

## 2.0 Interference of two Gaussian beams

### 2.1 Gaussian beam properties

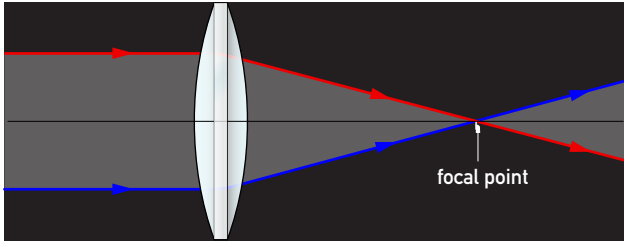
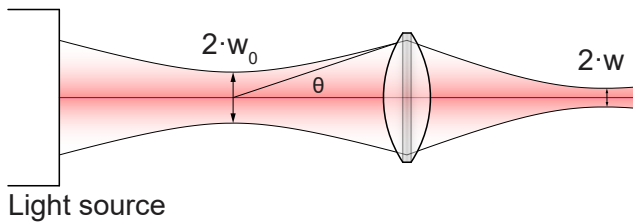


Fig. 1: Focusing of two beams according to geometrical optics

In reality, neither parallel light nor a focus with zero diameter exists. Thus, geometrical optics should only be used to provide an overview.



Light source

Fig. 2: Focusing a Gaussian beam

The Fig. 2 shows a more realistic illustration, instead of parallel beams, Gaussian beams with their respective beam waists are shown. To describe this reality in a more precise way we use the Maxwell's equations. To do so, we use the wave equation derived from the Maxwell equation:

$$\Delta \vec{E} - \frac{n^2}{c^2} \cdot \frac{\partial^2 \vec{E}}{\partial t^2} = 0$$

In this case we are only interested in the electrical field of the light since there are no interactions with magnetic dipoles in the propagation space.

Without restrictions the light would propagate as a spherical wave in all directions.

$$\vec{E} = \vec{E}(r) \text{ with } r^2 = x^2 + y^2 + z^2$$

When we consider the technically more important case of spherical waves propagating in the direction of  $z$  within a small solid angle we arrive at the following statement for the electrical field:

$$\vec{E} = \vec{E}(r, z) \text{ with } r^2 = x^2 + y^2 + z^2$$

In this case the solution of the wave equation provides electrical light fields which have a Gaussian intensity distribution over the cross-section, consequently called Gaussian beams. Similar to the solutions for the laser resonator, the Gaussian beams also exist in different modes depending on the implied boundary conditions. Such modes, especially the Gaussian fundamental mode ( $TEM_{00}$ ) are generated by lasers. However, the light of any light source can be considered as the superposition of different Gaussian modes. The intensity of a particular mode of a non coherent light source is small with respect to the overall intensity of it. For laser the situation is different, here the total light power can be contained in one fundamental mode. This is the most outstanding difference to ordinary light sources. How the

Gaussian beams behave differently from geometrical beams we will show in the following.

A Gaussian beam always has a waist. The beam waist radius  $w$  is a results of the solution of the wave equation as follows:

$$w(z) = w_0 \cdot \sqrt{1 + \frac{z^2}{z_R^2}} \quad (1)$$

$w_0$  is the smallest beam radius at the waist and  $z_r$  is named as the Rayleigh length

$$z_R = w_0^2 \frac{\pi}{\lambda} \quad (2)$$

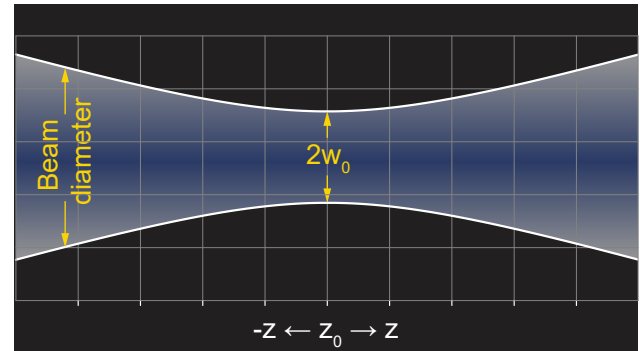


Fig. 3: Beam diameter as function of  $z$  of a Gaussian beam of a fundamental mode  $TEM_{00}$

The Fig. 3 shows the course of the beam diameter of a Gaussian beam as a function of  $z$ . At the position  $z = z_0$  the beam has the smallest beam waist. The beam waist size increases linearly with increasing distance. Gaussian beams are spherical waves thus a radius of curvature of the wave field to each point  $z$  can be attributed. This radius of curvature  $R$  (ROC) derived from the solution of wave equation is given by:

$$R(z) = z + \frac{z_r^2}{z} \quad (3)$$

This relation is illustrated in Fig. 4.

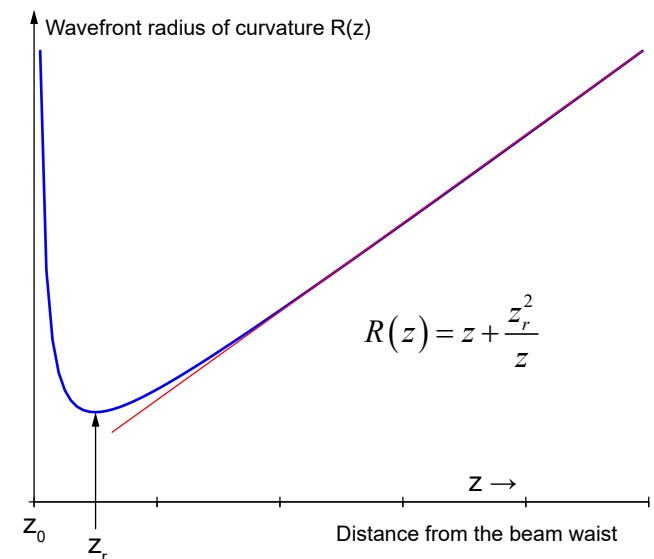


Fig. 4: The radius of curvature of the wave front as a function of the distance from the waist at  $z_0$

The ROC shows a minimum for  $z = z_r$ . For smaller values of

$z$  the ROC increases and for  $z=0$  it is infinite, that means the wave front is plane like for parallel waves. For higher values of  $z$  the radius of curvature increases linearly, indicated by the red line. This implies an important statement: a beam with infinite ROC (parallel beam) exists only in one point of the light wave, namely only in its focus. A not so strict interpretation defines a range for which the wave can be considered as parallel:

$$-z_r \leq z \leq z_r$$

The so defined Rayleigh range is shown in Fig. 5 as well as the far field ( $z \gg z_0$ ) divergence  $\Theta$  is shown as well.

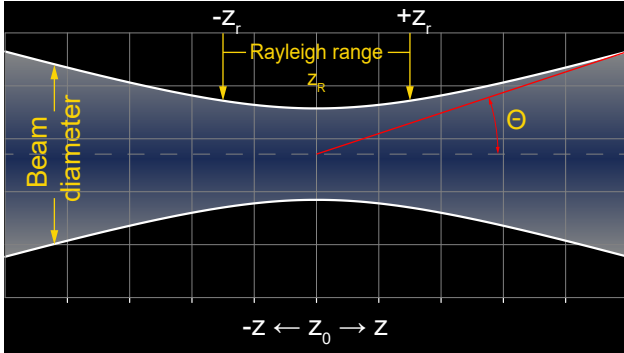


Fig. 5: Rayleigh range and far field divergence  $\Theta$

It should be mentioned, that the illustration of Fig. 5 does not reflect the real situation of a laser beam. The ratio of the Rayleigh range and the beam diameter is far apart from reality, but serves to explain these properties. To see how reality is, we consider, for example green laser pointer (532 nm) with a beam radius of  $w_0 = 1 \text{ mm}$  at the exit of the pointer. For the Rayleigh range  $z_R = 2 z_r$  we get:

$$z_R = 2 \cdot w_0^2 \frac{\pi}{\lambda} = 2 \cdot 10^{-6} \frac{3.14}{532 \cdot 10^{-9}} = 11,8 \text{ m}$$

That means that the ratio of the Rayleigh range to the beam diameter is  $11.8 / 0.002$  which yields 5900, which is impossible to illustrate in a graph.

The initial task is to treat the light waves as Gaussian waves and derive their properties. For an LDA to operate, we need to focus the light using a lens. The following considerations will give us an idea.

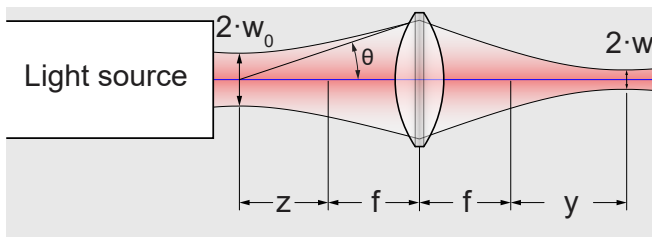


Fig. 6: Focusing a Gaussian beam

Fig. 6 shows the focusing of a laser beam with a lens with a focal length of  $f$ . The light source emits a beam with a divergence of  $\theta$  whereby the beam waist is located at the exit of the laser and the focusing lens in a distance of  $z+f$ .

The radius at the waist of the focused beam is given by:

$$w = \frac{w_0 \cdot f \cdot \theta}{\sqrt{w_0^2 + \theta^2 \cdot z^2}} \quad (4)$$

The location of the waist is given by:

$$y = \frac{z \cdot f^2}{z^2 + \left(\frac{w_0}{\theta}\right)^2} \quad (5)$$

For example, consider a laser pointer with a beam diameter of 1.5 mm and a divergence of 2 mrad. This beam is focused using a lens with a focal length of 50 mm at a distance of 2 meters from the laser. We can calculate the focused beam waist, denoted as  $w$ :

$$w = \frac{1.5 \cdot 10^{-3} \cdot 0.05 \cdot 2 \cdot 10^{-3}}{\sqrt{2.25 \cdot 10^{-6} + 4 \cdot 10^{-6} \cdot (2 - 0.05)^2}} = 35.9 \mu\text{m}$$

and for the location  $Y$  of the beam waist we find:

$$y = \frac{(2 - 0,05) \cdot 2,5 \cdot 10^{-6}}{(2 - 0,05)^2 + \left(\frac{1,5}{2}\right)^2} = 1.1 \text{ mm}$$

## 2.2 Gaussian beam interference

The following paragraph will derive the interference pattern of two crossing Gaussian beams.

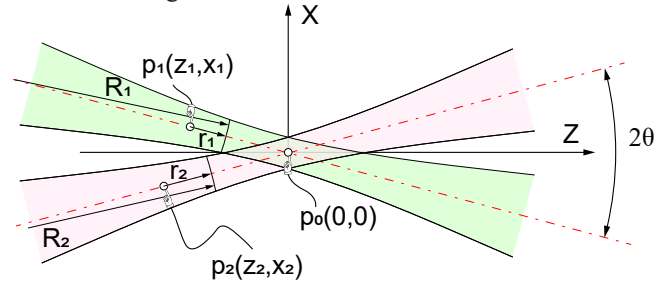


Fig. 7: Crossing of two Gaussian beams

$R_1$  and  $R_2$  are the radii of curvature,  $r_1$  and  $r_2$  the distance to the beam waist.

With the common equation of a circle

$$R^2 = x^2 + z^2$$

and the equation for the radius of curvature (ROC, ) we compose for the beam (1) the following equation:

$$\begin{aligned} [(z - z_1) + (R_1 - r_1) \cdot \cos(\theta)]^2 + \\ [(x - x_1) - (R_1 - r_1) \cdot \sin(\theta)]^2 = R_1^2 \end{aligned} \quad (6)$$

and for beam (2):

$$R_2 = r_2 \cdot \left[ 1 + \left( \frac{\pi \cdot w_0^2}{\lambda \cdot r_2} \right)^2 \right] \quad (7)$$

$$\begin{aligned} [(z - z_2) + (R_2 - r_2) \cdot \cos(\theta)]^2 + \\ [(x - x_2) + (R_2 - r_2) \cdot \sin(\theta)]^2 = R_2^2 \end{aligned} \quad (8)$$

From (6), (7) and (8) we gain the equations for the phase fronts of the beams in terms of  $r_1$  and  $r_2$ .

$$[r_1 \cdot (z - z_1) + r_0^2 \cdot \cos(\theta)]^2 + [r_1 \cdot (x - x_1) - r_0^2 \cdot \sin(\theta)]^2 = (r_0^2 + r_1^2)^2 \quad (9)$$

$$[r_2 \cdot (z - z_2) + r_0^2 \cdot \cos(\theta)]^2 + [r_2 \cdot (x - x_2) + r_0^2 \cdot \sin(\theta)]^2 = (r_0^2 + r_2^2)^2 \quad (10)$$

Constructive interference occurs in the overlap region when the phase difference is a multitude of the wavelength:

$$r_2 - r_1 = n \cdot \lambda$$

## 2.3 Fringe spacing

We are interested in the fringe spacing at the location  $z=0$  for two Gaussian beams which are crossing at their beam waists, for  $x_1=x_2=0$  and  $z_1=z_2=0$

With these conditions the analytical solution of (9) and (10) yields<sup>1</sup>:

$$X(n) = \frac{n \cdot \lambda}{2 \cdot \sin(\theta)} - \frac{n^3 \cdot \lambda^5}{16 \cdot \pi^2 \omega_0^4 \cdot \sin^3(\theta)}; n > 0$$

and for  $X(n)-X(n-1)$  we obtain the spacing of two neighbored constructive interference (fringe):

$$\Delta X(n) = \frac{\lambda}{2 \cdot \sin(\theta)} - (3 \cdot n^2 - 3 \cdot n + 1) \cdot \frac{\lambda^5}{16 \cdot \pi^2 \cdot \omega_0^4 \cdot \sin^3(\theta)}$$

The first term is well known from the planar wave model. The second term gives rise to deviations of the fringe separations, which we will neglect in the following considerations. We will use the first term to estimate the fringe separation with parameters of the later experimental setup.

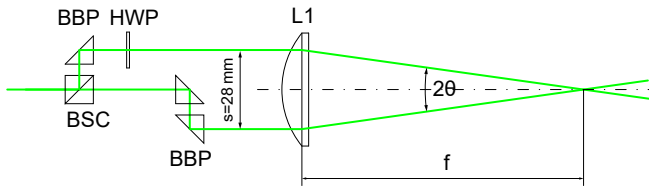


Fig. 8: Optical set-up of the LDA experiment

The collimated beam of the 532 nm diode-pumped solid-state laser (DPSSL) is divided by the beam splitting cube (BSC) into two beams of almost identical intensity. By means of 90° beam bending prisms, a lateral beam separation of 28 mm is achieved. After passing the focusing lens (L1), the two beams propagate under an angle of  $2\theta$  to each other. The angle  $\theta$  is derived by the following equation:

$$\tan(\theta) = \frac{s}{2 \cdot f}$$

whereby  $s$  is the lateral distance of the two beams and  $f$  the focal length of the lens (L1).

focal length $f$	Angle $\theta$ (°)	$\Delta X$ (μm)
100	8	1.9
200	4	3.8
300	2.7	5.7

Table 1: The fringe separation  $\Delta X$  for different focal lengths

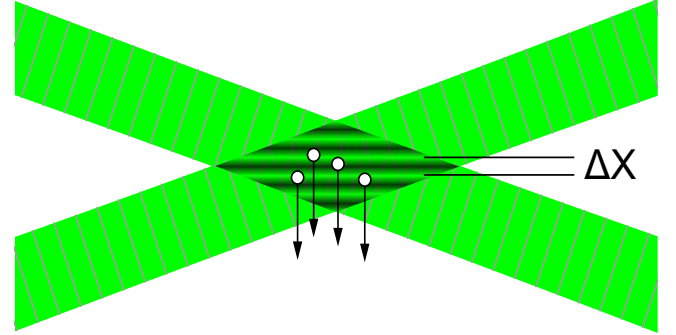


Fig. 9: Planar fringe model

The particles are moving through the zone of interference, and it is obvious that their size should be less than the fringe spacing to obtain a scattered light signal with high contrast. For good signal generation, the contrast of the fringes itself must be as high as possible. That means, in addition to the proper alignment of the beams, the size of the particles should be less than the fringe spacing.

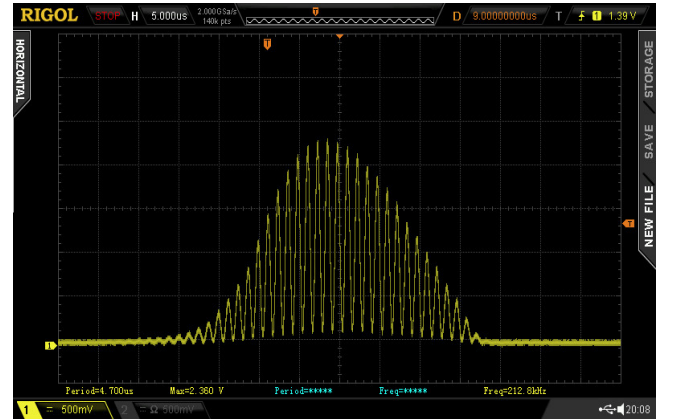


Fig. 10: Measured burst

The measured burst event (see page 15) has a length of 50 μs which corresponds to the beam waist at the jet position. The frequency of the burst is 212.8 kHz (measured from the oscilloscope) and is related to the fringe separation and speed of the jet flow.

<sup>1</sup> Enbang Li, Kiet Tieu, Mark Mackenzie, Interference Patterns of Two Focused Gaussian Beams in an LDA Measuring Volume, Optics and Lasers in Engineering, Volume 27, Issue 4, 1997, Pages 395-407, ISSN 0143-8166, [https://doi.org/10.1016/S0143-8166\(96\)00040-1](https://doi.org/10.1016/S0143-8166(96)00040-1).



### 3.0 Description of the components

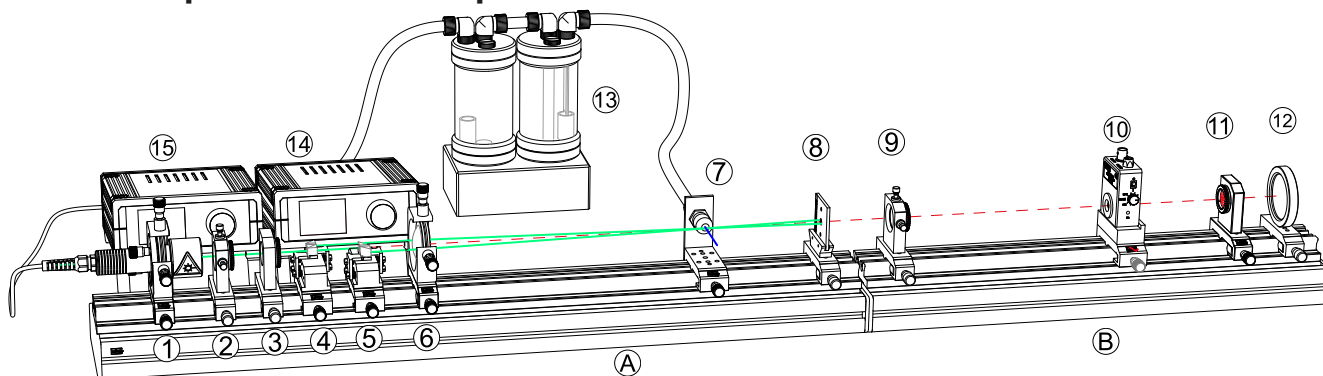


Fig. 11: LDA Set-up

#### 3.1 Optical rail (A,B)

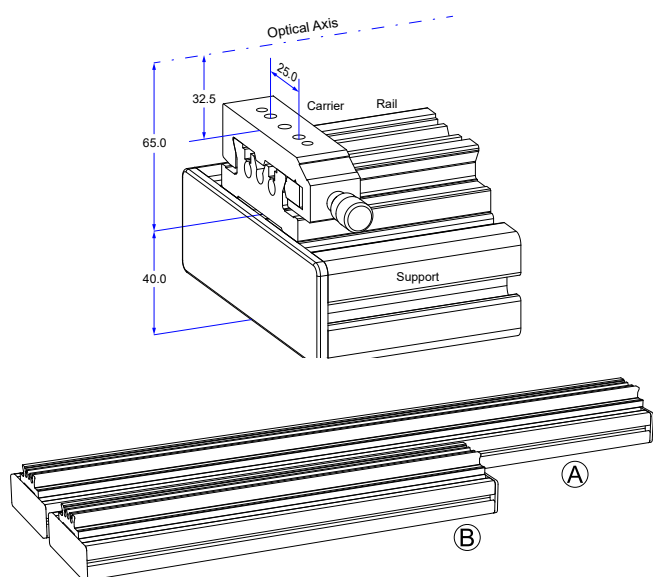


Fig. 12: Rail and carrier system

The rail and carrier system provides a high degree of integral structural stiffness and accuracy. Due to this structure, it is a further development optimized for daily laboratory use. The optical height of the optical axis is chosen to be 65/105 mm above the table surface. The optical height of 32.5 mm above the carrier surface is compatible with all other systems like from MEOS, LUHS, MICOS, OWIS and LD Didactic. Consequently, a high degree of system compatibility is achieved. The attached support elevates the working height above the table and significantly improves the handling of the components. In this set-up a 800 mm (A) and a 500 mm (B) rail is used.

#### 3.2 LQ-0040 532 nm stabilized Laser (1)

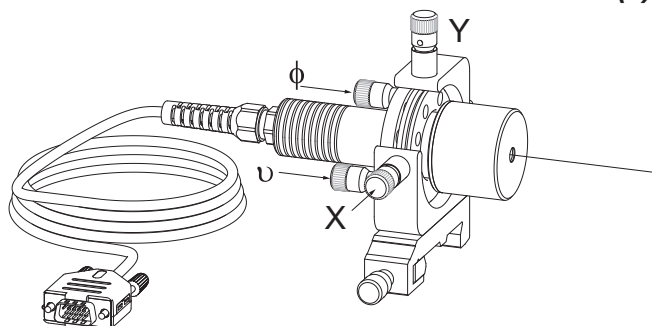


Fig. 13: LQ-0040 Green (532 nm) stabilized Laser, 40 mW

The laser module consists of a DPSSL (Diode-Pumped

Solid-State Laser) with second harmonic generation and can emit 40 mW at 532 nm. It is mounted in a 4-axis adjustment holder and controlled by the controller device (1).

#### Caution:

If no measures can be taken to avoid directly looking into the laser beam, the user should wear suitable laser safety goggles.

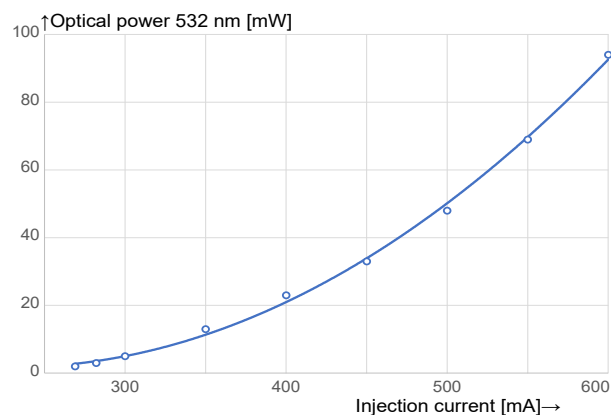


Fig. 14: Laser power versus injection current

The laser module consists of diode pumped Nd:YAG laser operating at 1064 nm with frequency doubling to 532 nm. In Fig. 14 the power of the frequency double radiation at 532 nm as function of the injection current of the pump diode. The typical quadratically relation can be recognized.

The green Laser Module (GLM) is mounted inside the housing between two Peltier elements. After connecting with the digital controller, the temperature can be set in a range from 10 to 35°C and is kept constant within 0.01°C. The line width of the GLM is less than 22 MHz, which can be proved by using the “LM-0300 Fabry Perot Spectral Analyser”. The maximum output power at 532 nm is 40 mW single mode and can be adjusted to a desired or recommended level.



### 3.3 Beam expander (2,3)

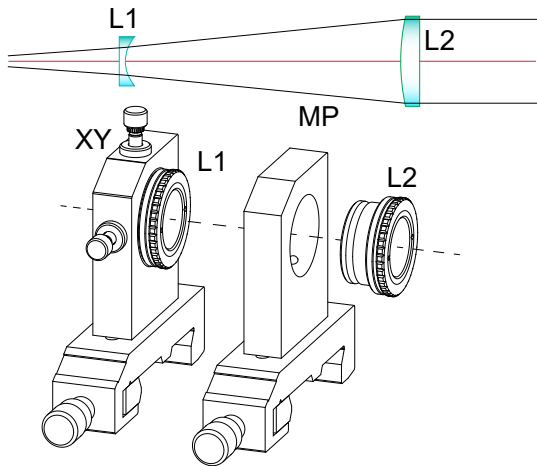


Fig. 15: Beam expander composed by (2) and (3)

The diameter of the green radiation emitted by the diode laser is very small, resulting in a strong divergence of the beam. To address this, the beam needs to be collimated and made parallel. This is achieved by using a combination of a concave lens (L1) with a focal length of -15 mm and a plan-convex lens with a focal length of 50 mm, both mounted in a C25 holder with a free aperture of 20 mm. The assembled lens is secured in a mounting plate (MP) using three spring-loaded steel balls that keep it in position. Additionally, the concave lens is placed in an XY adjustment holder (XY) to facilitate precise alignment of the beam direction.

### 3.4 Beam splitter unit (4)

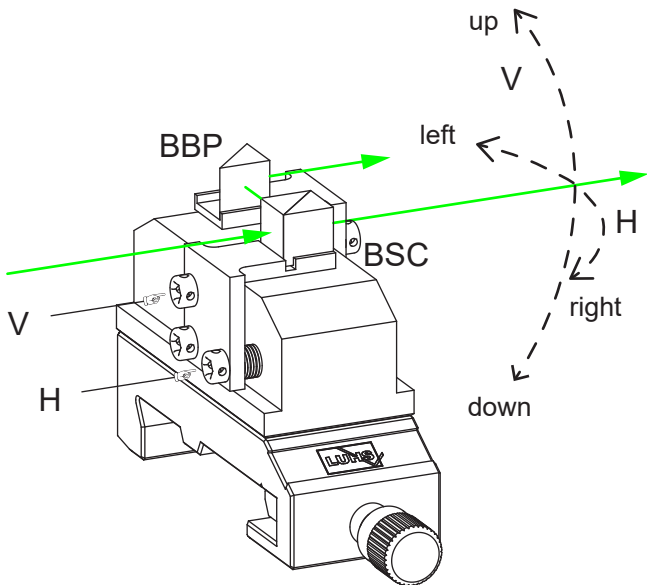


Fig. 16: Beam splitter unit (8)

The beam of the green laser passes the 50/50 beam splitter cube (BSC) and is divided into two beams with the same intensity. The deflected beam hits the beam-bending prism (BBP) and propagates with an offset of 14 mm parallel to the initial beam. The PBS, as well as the BBP, are mounted on adjustable stages. With capstan screws and a stack of cup springs, the displacement is achieved with long-term stability. A special tool is provided for the cross holes of the capstan screws.

### 3.5 Beam bender unit (5)

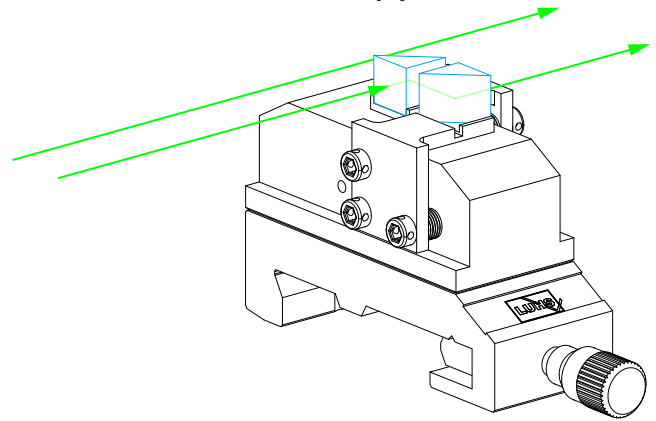


Fig. 17: Beam bender unit (10)

With two adjustable 90° prisms the direct beam of the laser is shifted by 14 mm apart from the central axis. With capstan screws and a stack of cup springs, the displacement is achieved with long-term stability. A special tool is provided for the cross holes of the capstan screws.

### 3.6 Focusing and bending lens (6)

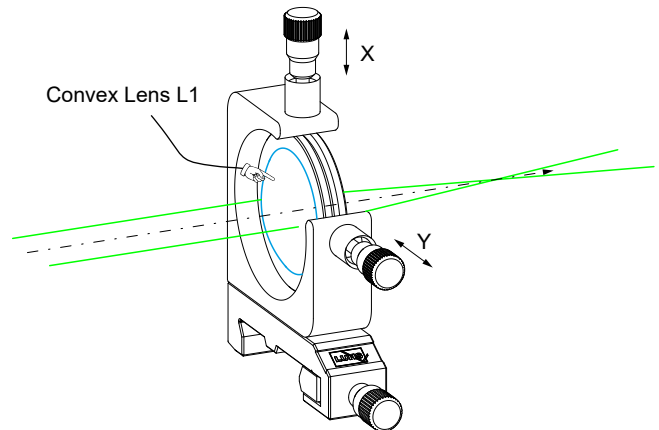


Fig. 18: Beam focusing and bending lens

The beam focusing and bending lens is mounted into an XY adjustment holder. With two fine-pitch screws, the location of the focus can be precisely aligned. The focal length is 300 mm.

### 3.7 Jet stream module (7)

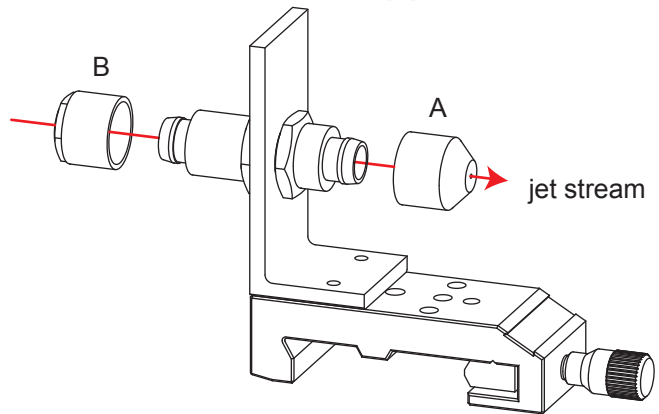


Fig. 19: Jet stream module with nozzle (A) and hose connector (B)

A set of four nozzles (A) with diameter 1, 2, 4 and 6 mm is provided. The individual nozzle (A) is screwed to the holder.

Experimental setup



### 3.8 Beam alignment aid (8)

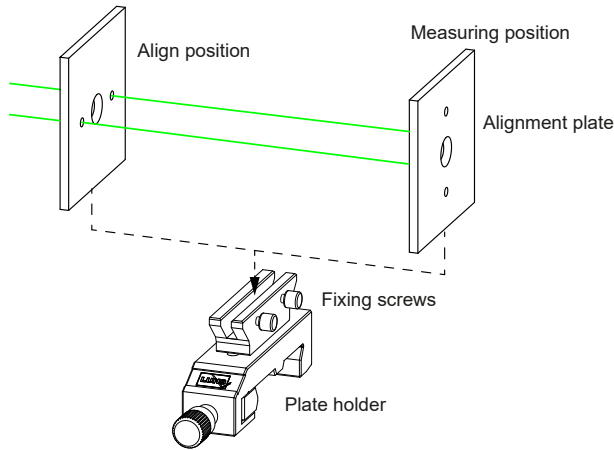


Fig. 20: Beam alignment aid and blocker

The alignment plate is placed into the plate holder, where it is held in position by two spring-loaded balls. In the align position, the two beams must pass undisturbed the holes, indicating proper alignment. In the measuring position, the alignment plate is turned 90° to block the two beams from reaching the photodetector.

### 3.9 Imaging lens (9)

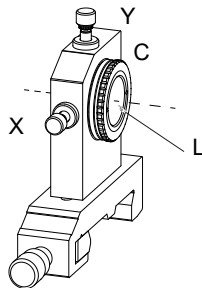
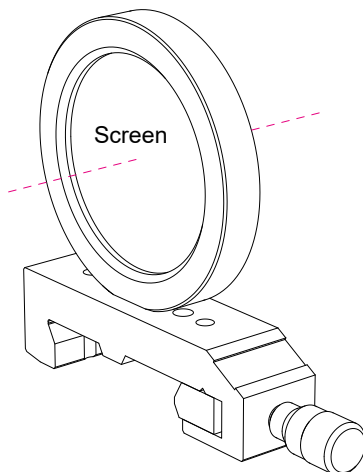


Fig. 21: Imaging lens to image the scattered light to the photodetector

The imaging lens (L) is secured in a click holder (C), which is then positioned within the XY adjuster. Fine-pitch screws are used to align the lens in the XY direction. With a focal length of 120 mm, the lens captures the scattered light from the LDA and directs it to the photodetector.

### 3.10 Display Screen (12)



A round sheet of translucent paper is mounted into a holder. The midpoint lies within the optical axis of the setup.

### 3.11 Crossed hair target screen (11)

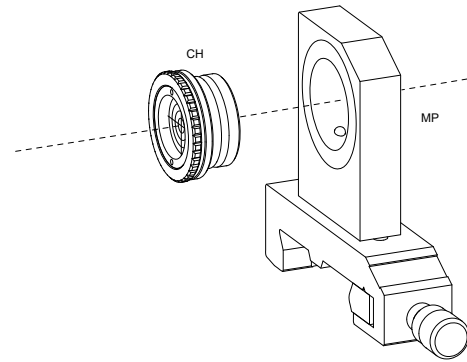


Fig. 22: Crossed hair target screen

A crossed hair target screen is part of a 25 mm click mount (CH) that can be inserted into the mounting plate (MP). Three precision spring-loaded steel balls keep the screen in position. It is used to visibly align a light beam concerning the optical axis of the rail and carrier system.

### 3.12 Fast photodetector (10)

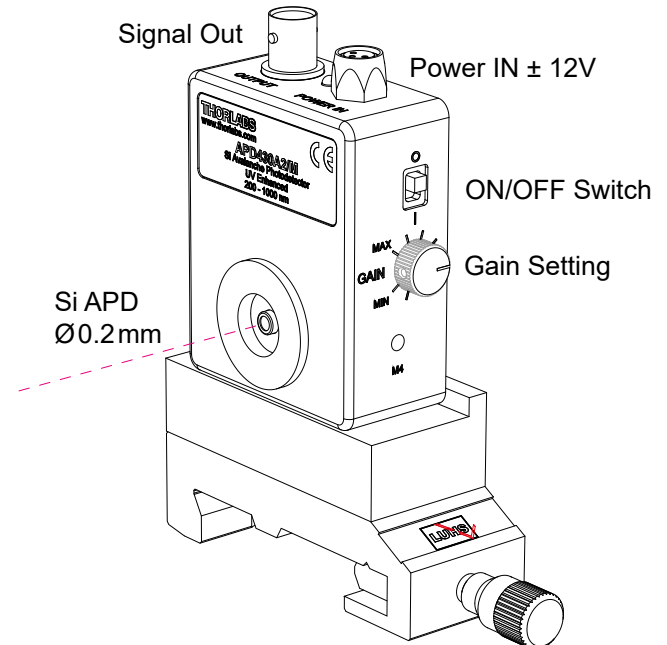
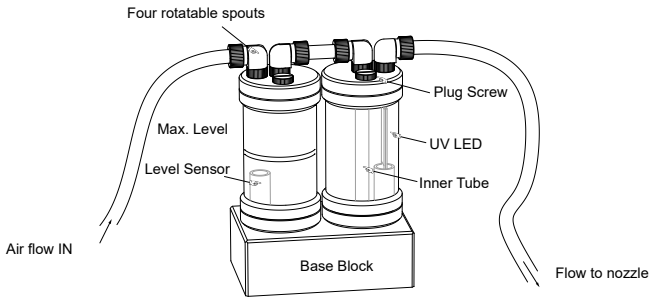


Fig. 23: Avalanche Photodetector

The Thorlabs APD430A2 series of temperature-compensated Avalanche Photodiodes combine a high sensitivity Si or Avalanche Photodiode with a specially designed ultra-low noise transimpedance amplifier for detection of optical signals from DC to 400 MHz.

The Avalanche Photodiodes cannot be damaged by unwanted ambient light, which is an advantage over many photomultiplier tubes. The APD430A2 feature a continuously adjustable Gain that is based on the adjustment of the APD's M (multiplication) factor. They also incorporate a special electronic circuit to compensate for the temperature dependency of the M factor. The APD430A2 is powered by the included external power supply LDS12B ( $\pm 12$  VDC, 250 mA) via a PICO M8 power connector.

### 3.13 LDA Particle Generator (13)



**Fig. 24: MM-L100 LDA Particle Generator**

The bottom of the left glass cylinder houses an ultrasonic nebulizer of type NB-80E-01-H. It operates within a frequency range of 2.35 to 2.50 MHz and produces a nominal 150ml/h. Due to the high ultra-sound frequency, micro-particles with a diameter of 3 μm are generated. The connected controller allows the variation from 0 to 100 % of the mist generation. The generated mist is blown by an air stream from the left tank into the right one, where it passes a tube to condense larger droplets at its wall. Inside the right tank, an array of LEDs emit deep UV radiation at 270 nm to disinfect any germs, if any. The clean and dried mist leaves the tank to the nozzle.

A soft silicone hose (12 mm x 1 mm) connects the left tank to the controller’s blower and is clamped to a rotatable spout at the tank. A soft silicone hose (12 mm x 1 mm) connects the left tank to the controller’s blower and is clamped to a rotatable spout at the tank. Two rotatable spouts connect the left tank to the right tank with a short, soft silicone hose.

To fill or empty the left tank, the plug screw needs to be removed. With the provided pipette, only distilled water is filled in or removed.

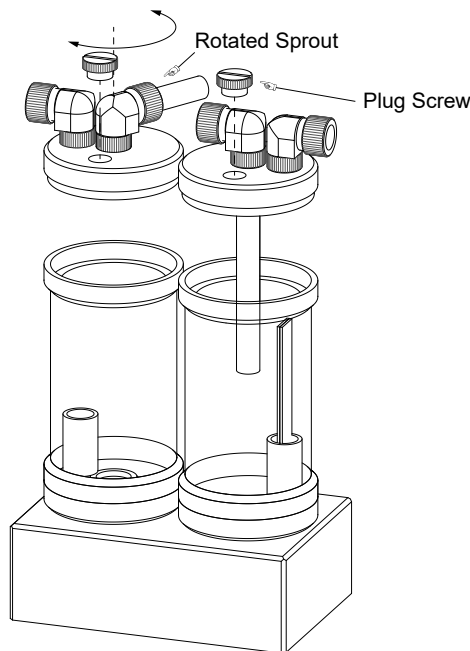


**Fig. 25: Dissembled Particle Generator**

If the device is not in use for a longer time, it is recommended that the water is removed completely. To do this, release the swivel nut of the spout and turn it until the hose is disconnected. Unscrew the tank’s top and store the device upside down to let the excess water rinse off.

### 3.14 DC-0320 US particle generator (15)

The US particle generator controller operates the nebulizer of the MM-L100 particle generator. It monitors both the water level and temperature. The device includes a blower whose speed is regulated by PWM (Pulse Width Modulation). The controller features a touch panel for selecting parameters and a setting knob for adjusting the desired value.



**Fig. 26: Front view of the US Particle Generator Controller**



**Fig. 27: Rear view**

The device operates using a supplied 12V/2A power supply. The MM-L100 particle generator is connected via a 9-pin subD connector, and the blower output fits a 12mm soft silicone hose.

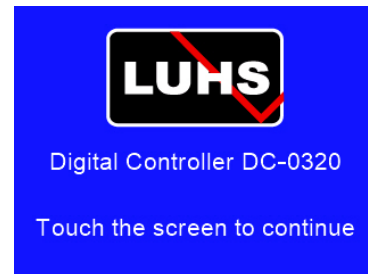


**Fig. 28: Start screen**

After switching on the DC-0320 device, the start screen appears and informs about the model name. Touching the screen brings up the main window.

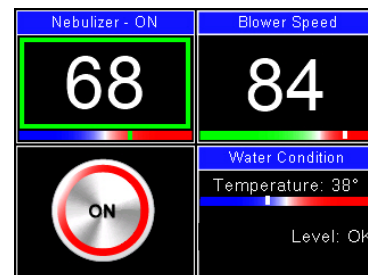


**Fig. 29: Main screen**

When you touch the entry field on the Nebulizer, a green frame appears to indicate your selection. You can adjust the settings by turning the knob, which changes the value within a range of 0 to 100. To set the “Blower Speed,” simply touch its entry field; this setting also ranges from 0 to 100.

The blower speed is applied instantly, while the Nebulizer itself must be activated by pressing the ON/OFF button. The Water Condition field displays both the level and temperature of the water.

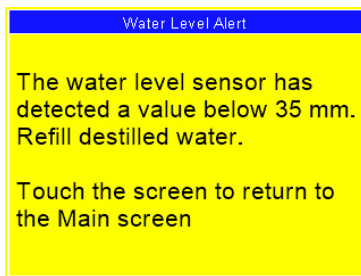


Fig. 30: Water Level Alert

The nebulizer tank's water level is monitored. If it drops below 35 mm, the nebulizer will automatically turn off. It can only be switched back on after refilling the tank above 35 mm.

### 3.15 Digital Diode Laser Controller (14)



This microprocessor operated device contains a laser diode controller and a temperature controller driving the Peltier element of the attached diode laser. A touch panel display allows in conjunction with the digital knob the selection and setting of the parameters.

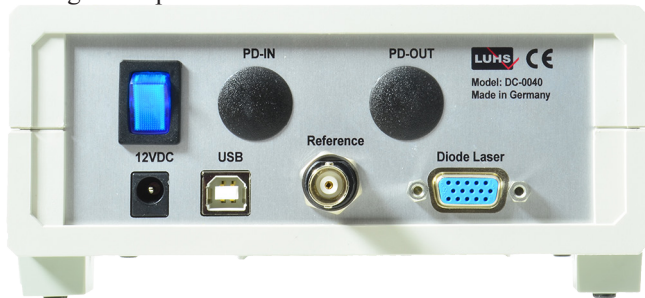


Fig. 31: Digital Diode Laser Controller MK1

The laser diode module is connected via the 15 pin HD SubD panel jacket. The controller reads the EEPROM of the laser diode and sets the required parameter accordingly. The MK1 is powered by an external 12V/ 1.5 A wall plug supply. A USB bus allows the connection to a computer for remote control. Furthermore, firmware updates can be applied simply by using the same USB bus.

The MK1 provides an internal modulator which allows the periodic switch on and off of the diode laser. A buffered synchronization signal is available via the BNC jacket (MOD). Furthermore, the duty cycle of the modulation signal can be varied in a range of 1...100 % to enable the measurement of thermal sensitivity of the optically pumped laser crystal. When the LED or laser is operated in modulated mode, the reference modulator signal is available at the "REFERENCE" BNC connector. Further detailed specifications are given in the following section of the operation software.

#### 3.15.1 Diode laser controller screens

When the external 12 V is applied, the controller starts displaying the screen as shown in the figure below.

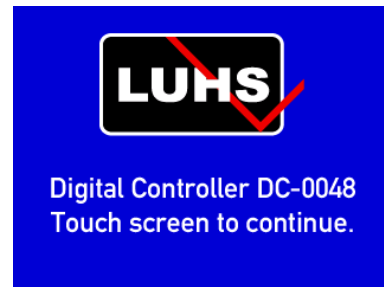


Fig. 32: Start screen

#### 3.15.2 Laser Safety

The first interactive screen requires the log in to the device since due to laser safety regulations unauthorized operation must be prevented. In general, this is accomplished by using a mechanical key switch. However, this microprocessor operated device provides a better protection by requesting the entry of a PIN.

After entering the proper key, the next screen is displayed and the system is ready for operation.



Fig. 33: Authentication screen

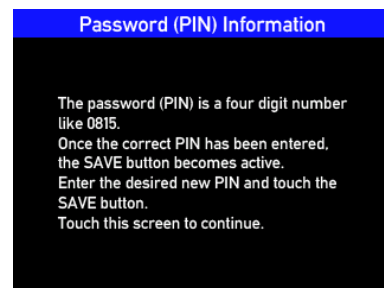
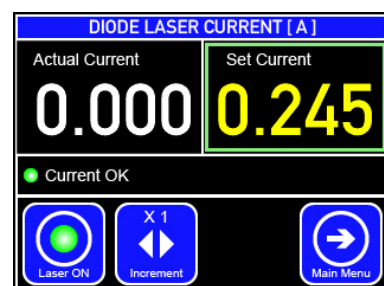


Fig. 34: Information for the password

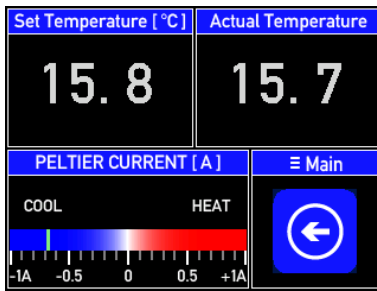
#### Diode Laser Settings



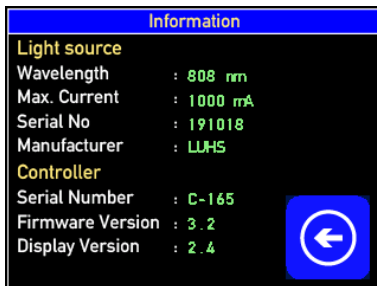
To change the set current of the diode laser, touch the "Set Current" window. Once activated it is framed with a green border. By turning the settings knob (SET) the desired value is selected. For faster settings of the current in 10 mA instead of 1 mA the increment button is touched. Touch the "LASER ON" to switch the laser on. The PID controller is

activated and drives the laser slowly to the desired value. This may take a few seconds to reach the set value. For immediate “Laser OFF” just touch Laser ON button.

### Temperature Screen

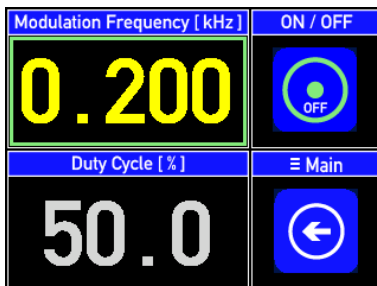


From 2023 on, the temperature settings are disabled since the temperature has a negligible influence on the wavelength. The laser diode is passively cooled and the actual temperature is displayed here.



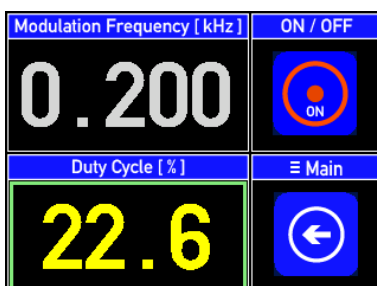
When tapping the Device Info button of the main screen this screen comes up. It again reads and displays the information stored in the EEPROM of the attached diode laser. If an entry exceeds the maximum or minimum limit value retrieved from the EEPROM of the attached diode laser the entry is reversed to the respective minimum or maximum value.

### Modulation settings



The diode laser can be switched periodically on and off. This is for a couple of experiments of interest. By tapping the display of the modulation frequency, the entry is activated. Turning the settings knob will set the desired frequency value. The modulation becomes active, when the Modulator ON/OFF button is tapped.

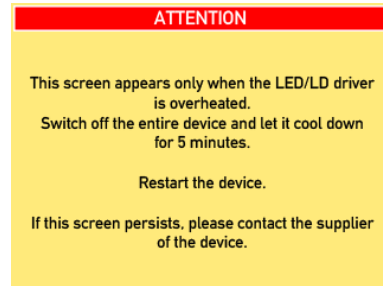
### Duty Cycle settings



For some experiments it is important to keep the thermal

load on the optically pumped laser crystal as low as possible or to simulate a flash lamp like pumping. For this reason, the duty cycle of the injection current modulation can be changed in a range of 1...100 %. A duty cycle of 50% means that the OFF and ON period has the same length. The set duty cycle is applied instantly to the injection current controller.

### Overheating warning



This screen you should never see. It appears only when the chip of the injection current controller is over heated. Switch of the device, wait a couple of minutes and try again. If the error persists, please contact your nearest dealer.



This screen is self-explanatory and appears either when no laser diode is connected or the data reading from the EEPROM is erroneous.



## 4.0 Set-up and alignment

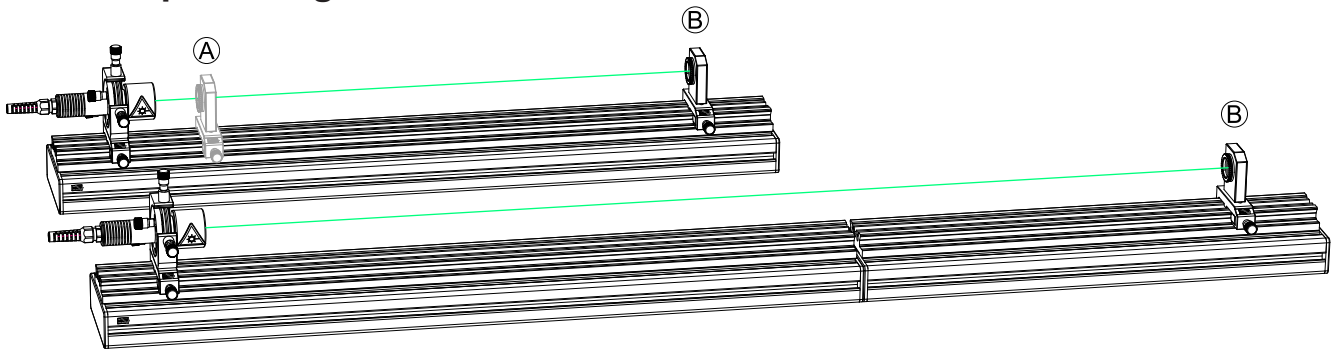


Fig. 35: Setup Step 1

Place the optical bench, which is 800 mm long, on the work table. Note that the bench has four silicon rubber feet that adhere to the table's surface; remember to lift the bench before moving it. Position the diode laser and switch it on at the lowest optical power setting. Place the crossed hair target near the end of the bench and align the laser spot with the horizontal adjustment screws so that it is centered on the target. Move the target closer to the laser and use the verti-

cal adjustment screws to center the beam. Return the target to position B and repeat the alignment process. 6. Continue adjusting until the beam is centered in both positions. Add the 500 mm length bench to the table, butting in line against the 800 mm long bench. Place the crossed hair target almost at the end of the 500 mm bench and check that the beam hits the center of the target.

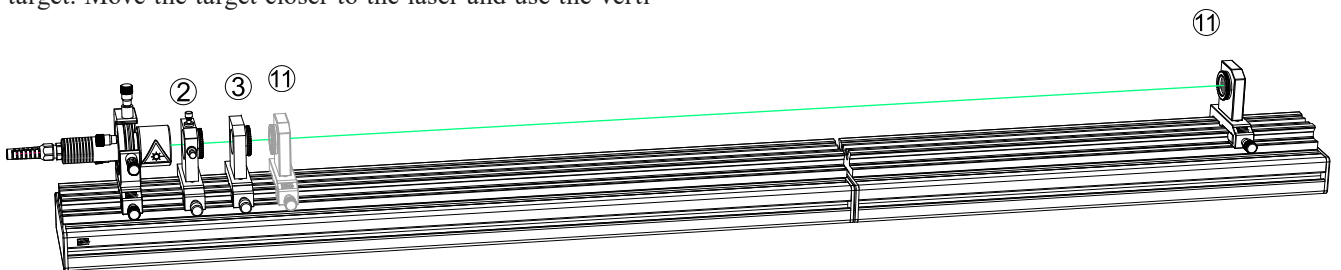


Fig. 36: Align beam expander (2,3) for parallel beam

Place the first element of the beam expander (lens 2) approximately 1 to 2 cm away from the laser. Next, position the second element (convex lens 3) about 2 cm away from the first element. Align the first element so that the laser beam hits

the center of the crosshair target (11). Then, gently adjust the second element to achieve the most parallel beam possible from the green laser. Finally, ensure that the beam is aligned with the center of the target at both the near and far positions.

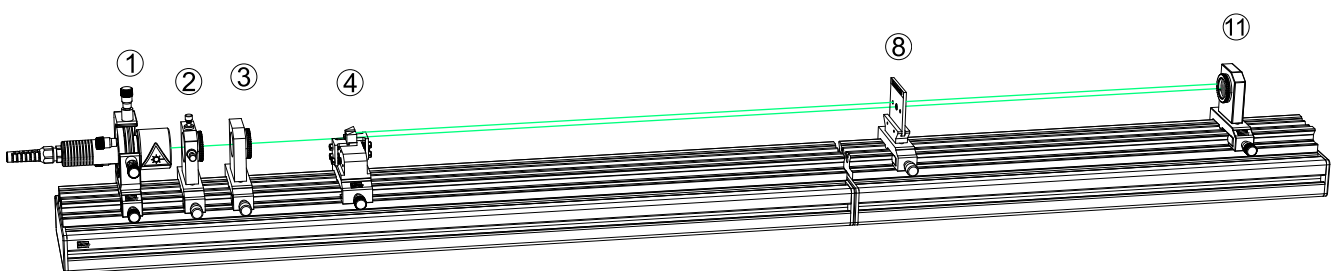


Fig. 37: Insert the beam splitter and displacer (4)

Once the green laser beam is parallelized and centered on the optical axis, we insert the beamsplitter unit (4). This unit functions as both a beam splitter and a deviator, with a parallel offset of 14 mm. The central beam should pass through

the alignment aid (8) and strike the target at its center. If the beam does not hit the target correctly, the beamsplitter cube and the bending prism can be adjusted to achieve proper alignment.

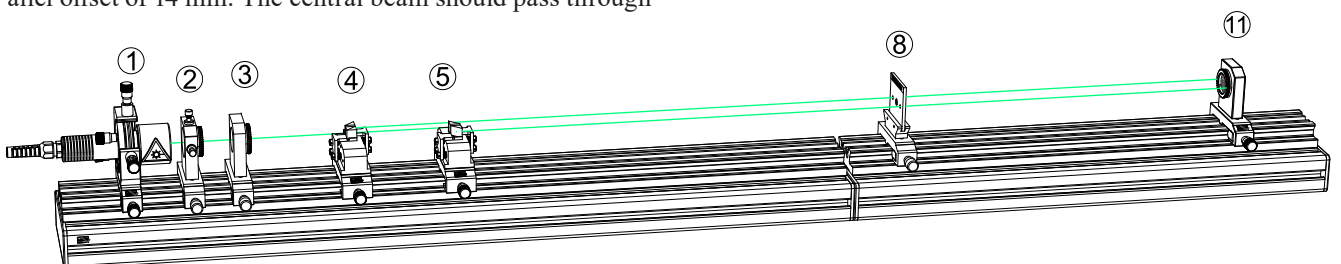


Fig. 38: Insert the beam bender unit (5)

The beam bender unit (5) is located next to the beamsplitter unit (4). It shifts the central beam by 14 mm, creating two beams that are 28 mm apart. The newly created beam passes

through the alignment aid via the second hole. The direction of this beam can be adjusted using the beam-bending prisms. Both beams must pass through the alignment aid (8), which should be verified at both near and far positions.

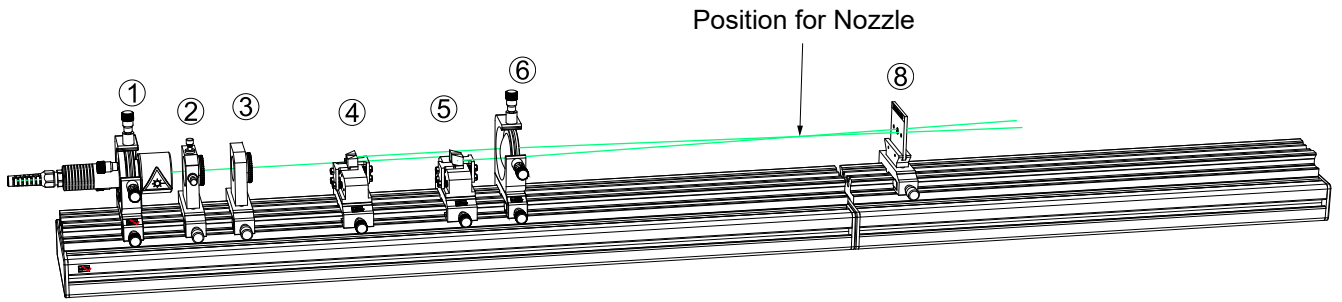


Fig. 39: Placing the beam focusing lens

Immediately following the beam bender unit (5), the focusing lens is positioned. This lens bends the two beams, which intersect at the focal length of 300 mm. Additionally, the beams are

tightly focused and overlap to produce the necessary interference. The nozzle is located at the point where the beams cross.

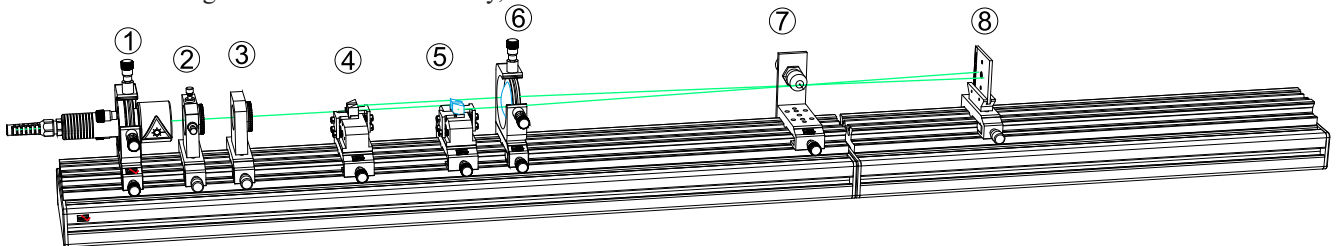


Fig. 40: Location of the nozzle

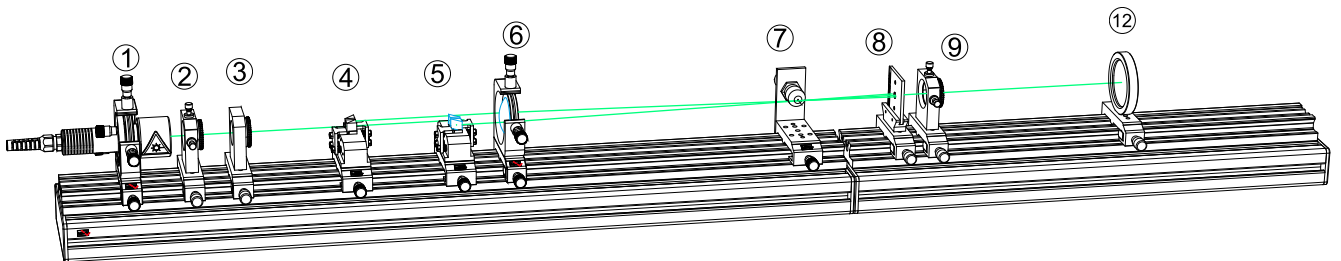


Fig. 41: Checking the focus of the jet image



Fig. 42: Screen image (12) with (left) and without jet stream

After turning on the laser and setting the nebulizer to its maximum blower speed and power, a strong jet and strong scattered light is produced and captured on the image screen (13). Next, rotate the alignment aid (8) by 90 degrees to block the main beams, and position the imaging lens behind it. Adjust the image screen (12) until a clear spot appears in the center (as shown in the left image of Fig. 42). Finally, verify whether the spot disappears when the jet is blocked or switched off (right image of Fig. 42).

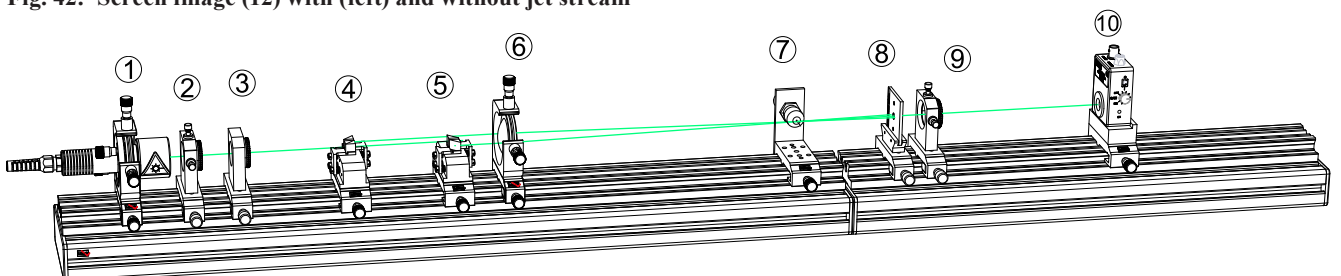


Fig. 43: Place the photodetector (10)

Observe the location of the image screen (12) and replace it with the APD module (10). By adjusting the imaging lens (9) in the XY direction, center the image spot on the avalanche photodiode (APD). Carefully reposition the APD module to align it to the focus of the jet image.



## 5.0 Measurements

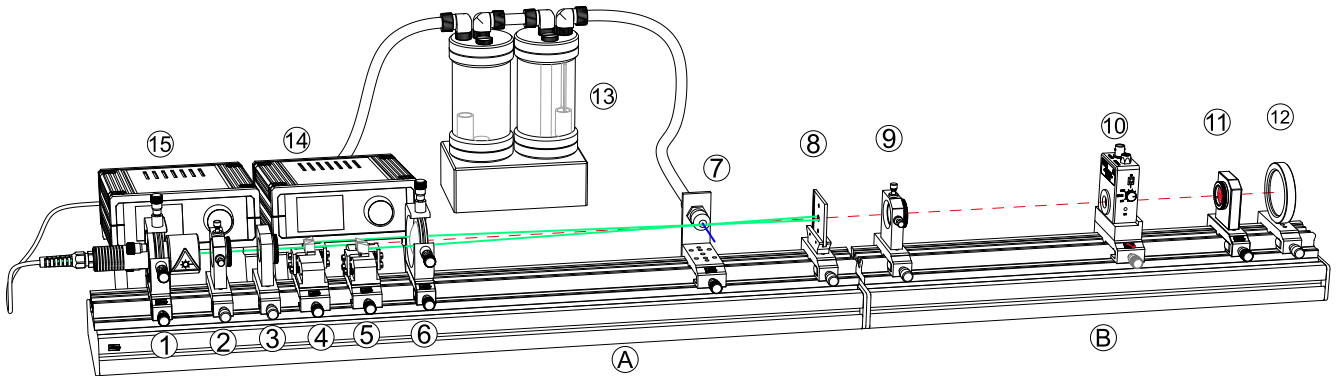


Fig. 44: Final set-up

Connect the APD module to its power supply and attach the output to an oscilloscope. At first, you will observe a scrambled signal. Carefully move the nozzle back and forth while monitoring the oscilloscope screen. In a specific position, you will notice some curling in the signal, which indicates

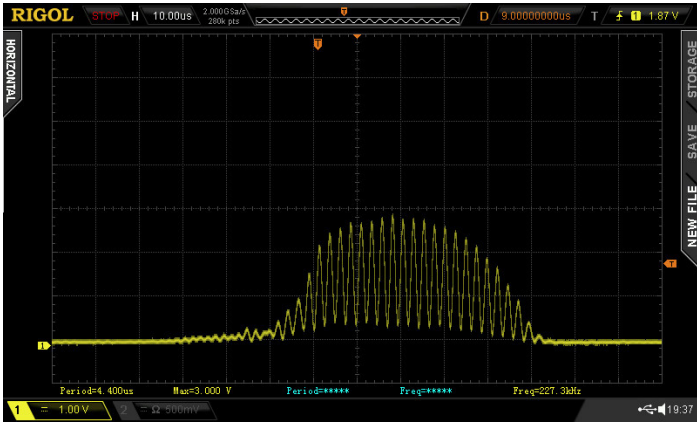
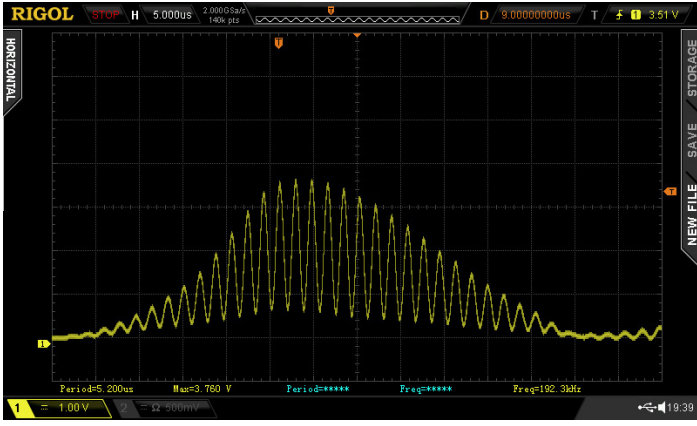
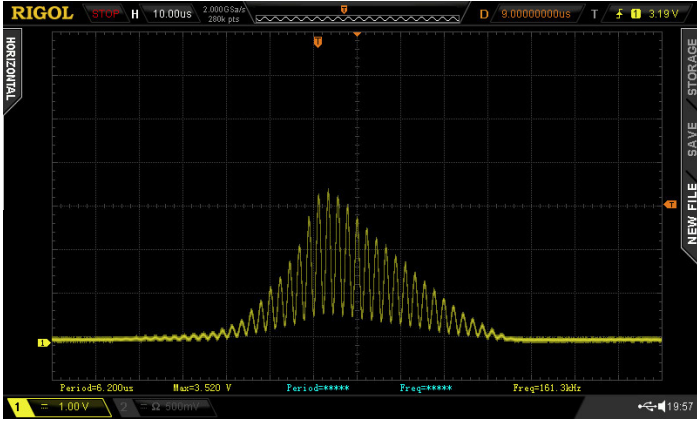
the optimal position of the jet. Ensure that both beams overlap in this area. To enhance the overlap, make slight adjustments to the prisms of the beam bender (5) until you achieve maximum curling.

### 5.1 Example of Measurements

The table presents a small collection of measurements. The nozzle diameter was 2 mm, the laser power was set to 400 mA, and the temperature of the laser was adjusted to 29.4°C. Images from the oscilloscope were captured for various nebulizer powers and blower speeds. The oscilloscope's trigger level was configured to 3/4 of the anticipated burst height,

with the trigger mode set to single. The trigger level is indicated by a red arrow on the right side of the oscilloscope image, and the duration of each deviation is displayed at the top. The length of a burst event varies based on the blower speed, ranging from 50 to 80  $\mu$ s, while the burst frequency fluctuates between 80 kHz and 250 kHz.

Nebulizer (0..100)	Blower (0..100)	
70	53	
70	40	

Nebulizer (0..100)	Blower (0..100)	
70	70	
70	80	
80	100	
50	100	